Proceedings of the ASME 2015 Dynamic Systems and Control Conference
DSCC 2015
October 28-30, 2015, Columbus, USA

DSCC2015-9919

A NEW CONTINUUM ROBOT WITH CROSSED ELASTIC STRIPS: EXTENSIBLE SECTIONS WITH ONLY ONE ACTUATOR PER SECTION

Andria A. Remirez*
Department of Mechanical Engineering
Vanderbilt University
Nashville, Tennessee 37235
Email: andria.a.remirez@vanderbilt.edu

Robert J. Webster III
Department of Mechanical Engineering
Vanderbilt University
Nashville, Tennessee 37235
Email: robert.webster@vanderbilt.edu

ABSTRACT

We propose a new kind of continuum robot based on crossed elastic strips. The actuator-specified location of the crossover point controls the lengths of the sections, enabling a wider range of configurations than would be possible with traditional fixed-section-length robots. Push-pull actuation of the crossed strips controls the curvature of the sections. We provide a model that describes the resulting configurations in terms of tangent circular arcs of varying lengths. Experiments with a prototype yield tip positions that agree with model predictions with an average error of 4.6% of the robot's length.

INTRODUCTION

Continuum robots have unique properties among robotic manipulators. Their passive compliance and ability to take on a variety of shapes make them particularly well-suited to tasks in which they must operate in a delicate environment or maneuver around obstacles [1–3]. A variety of designs for continuum manipulators have been proposed, including pneumatically and hydraulically actuated manipulators [4–8], tendon-driven arms [9–13], designs with flexible push-pull actuation rods [14], and manipulators whose motion arises from the elastic interaction of flexible pre-curved concentric tubes [15, 16]. A typical design scheme among continuum robots involves multiple similar, individually actuated continuum sections, assembled in series to produce a multi-section arm.

The ability to vary the length of the individual sections within a continuum robot is desirable, since it expands the range of shapes the robot can achieve [17]. However, the mechanical design and implementation of robots with this capability can be challenging for nearly all continuum robot designs. Perhaps the lone exception is pneumatic arms, since many pneumatic manipulators are inherently extensible [3]. However, pneumatic designs are not ideal for all tasks, and do not scale down to small sizes as well as some other designs [18]. When smaller diameters (on the order of several millimeters, for example) are required, tendon- and rod-actuated designs are often selected. These designs typically have fixed backbone lengths for each section. However, there has been some research toward making them extensible. In [19], Blessing and Walker present a prototype of a tendon-driven robot whose section lengths can be adjusted and set prior to actuation, but not varied in real-time during robot operation. In this paper we present a design where the relative lengths of two sections can be varied during robot operation by the robot's actuators. We also provide a model for this robot based on the constant curvature assumption.

Constant curvature kinematic models which accommodate variable section lengths have been developed for general extensible multisection arms in [20–22]. Indeed, for some classes of continuum robots, extending fixed-section-length models to allow for varying section lengths is as simple as treating section length parameters as inputs rather than constants [19]. The notion of variable section lengths has also been used to model unintended length changes, which may occur in response to tendon-applied loads on the backbone, as in [12].

The new variable-section-length design we propose here is

*Corresponding author.

inspired by the work of Yamada et al. in [23]. They propose a mechanism of bending for a small-scale continuum manipulator which can enable a variety of unusual robot shapes. The concept involves two flexible strips which are attached together at one end, crossed over one another one or more times, and inserted into a flexible outer sheath. Translating one of the strips into or out of the sheath causes the strips to push on the walls of the sheath and bend it into a curved shape.

The key innovation in our design in contrast to that of Yamada et al. is to provide direct actuator control of the location of the crossover point. This provides improved control over the shape of the device, and enables a greater variety of achievable shapes. Coupling the location of the change in curvature to an input also has the benefit of enabling the use of the simple piecewise constant curvature kinematic model we present in this paper. Through experiments with a 4.5 mm diameter prototype, we demonstrate that the model can predict manipulator tip position to within an average of 4.6% of the robot's length across a wide range of crossover point locations.

MANIPULATOR DESIGN

The manipulator design concept is illustrated in Figure 1. Its key components are (a) a flexible outer sheath of length L and inner diameter d, (b) a pair of two elastic strips, and (c) a spacer disc (hereafter referred to as the crossover disc) which constrains the strips to cross to opposite sides of the sheath at a specific point along the length of the robot. The tip disc (d) is affixed to the ends of each of the two strips, and also to the tip of the outer sheath. The strips are able to slide through their respective slots in the crossover disc. Also at the crossover disc, two thinner, less stiff strips are affixed to the disc. When one of the thicker strips is inserted or retracted, the robot bends into two curves, opposite in direction, whose relative lengths are defined by the crossover disc location. Pushing or pulling on the two thinner strips together provides translational motion of the crossover disc, thereby changing the location of the point of curvature change between the two sections.

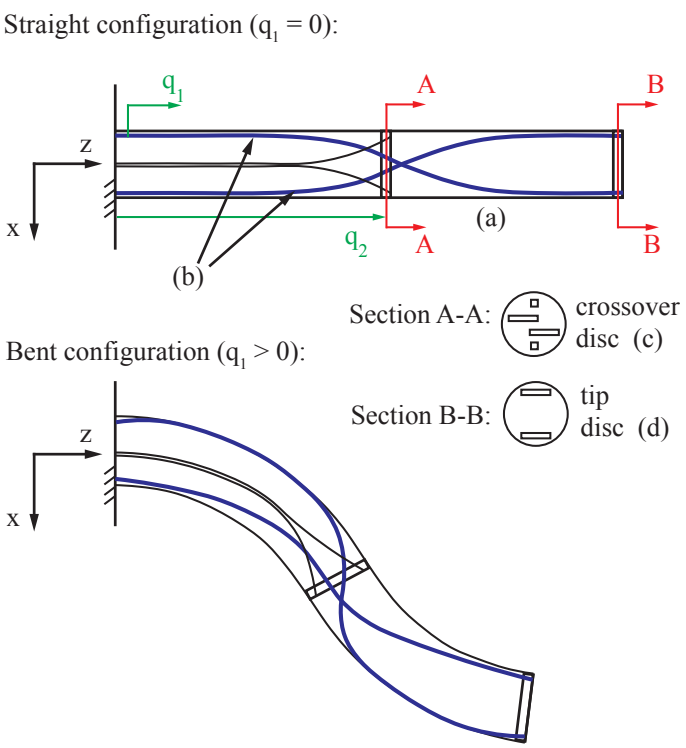

FIGURE 1: Illustration of manipulator design concept. The flexible outer sheath (a) contains a pair of bending strips (b). These strips are shown at a side view (i.e. the view is of their shorter cross-sectional dimension). The strips slide through the crossover disc (c) and are affixed to the tip disc (d).

FIGURE 2: Photograph of experimental prototype, with the plastic covering removed.

Experimental Prototype

A small-scale prototype of the manipulator is shown in Figure 2. Its length is 78 mm and its outer diameter is 4.5 mm. The outer sheath is composed of a flexible compression spring, wrapped in a flexible thin film of polyurethane medical tape (not shown in Figure 2). The inner diameter of the spring is 4 mm. The polyurethane covering is attached to the spring itself as well as to the tip disc via its adhesive backing.

Each of the bending strips is a segment of 1.52 mm by 0.29 mm nitinol strip, while the two strips used to translate the crossover disc are 0.51 mm by 0.28 mm nitinol strips. These thinner strips are routed around one side of the two bending strips, meeting in the center of the cross-section at the base. Both the tip disc and the crossover disc are 3.6 mm in diameter and were laser cut from 1.28 mm thick Delrin plastic. The bending strips are attached to the tip disc via J-B Weld epoxy, and the smaller strips are attached to the crossover disc with a cyanoacrylate adhesive. To further aid sliding of the bending strips within the crossover disc, the strips were coated with a PTFE dry lubricant spray.

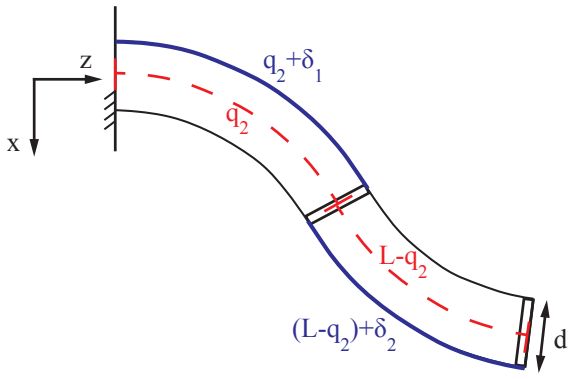

FIGURE 3: Illustration of kinematic model parameters.

KINEMATIC MODEL

A simple geometrically derived kinematic model can be used to approximately predict the shape of the robot as a function of the actuation variables q_1 (translation of one of the bending strips) and q_2 (arc length along the robot at which the crossover disc is located).

The primary underlying assumptions used to generate the model are that the robot's length L is much greater than its diameter d, that out-of-plane motion is small since the two strips are close to one another (producing little torque about the long axis of the robot), and that frictional effects are negligible. We assume that the shape is composed of two constant curvature (i.e. circular) arcs tangent to one another at the location of the crossover disc. The first circular arc is assumed to leave the base in a direction perpendicular to the base plate. One strip is chosen to remain fixed, while the other is chosen to be translated in and out as the input q_1 is applied.

As the actuated strip is inserted, it bends and comes into contact with the edges of the sheath, causing the sheath to bend into two opposing arcs. Withdrawing the strip creates the opposite effect, in which the other, fixed strip presses against the opposite walls. We assume that the differences in the lengths associated with the regions of the strip near the crossover disc that are *not* in contact with the wall do not significantly affect the overall robot shape. In other words, we model the robot as though the longer strip comes into contact with the sheath at the outside edge of each curve along the entire length of the robot, such that its crossing at the disc is discontinuous and instantaneous, as shown in Figure 3. This and other assumptions will be examined experimentally in later sections where we compare the predictions of this model to experimental data from our prototype.

To derive a geometric model for the device, first consider the case where q_1 is positive. With the centerline of the robot assumed to be a constant length, the centerline arc lengths of the proximal circular section (ℓ_1) and that of the distal circular section (ℓ_2) are defined by:

$$\begin{aligned} \ell_1 &= q_2 \\ \ell_2 &= L - q_2. \end{aligned} \tag{1}$$

In determining the resulting curvatures of each of the two sections, we assume that the inserted length q_1 becomes distributed along the two arc lengths directly in proportion to the relative lengths of each section. Thus the increase in the lengths of the outer edge of section 1 (δ_1) and the outer edge of section 2 (δ_2) are:

$$\begin{aligned} \delta_1 &= \left(\frac{\ell_1}{L}\right) q_1 \\ \delta_2 &= \left(\frac{\ell_2}{L}\right) q_1. \end{aligned} \tag{2}$$

Based on this assumption, the following relationships between arc length (ℓ_i), radius of curvature (r_i), and subtended angle (θ_i) can be written for the centerline of each of the two sections:

$$\begin{aligned} r_1\theta_1 &= q_2 \\ \left(r_1 + \frac{d}{2}\right)\theta_1 &= q_2 + \delta_1 \\ r_2\theta_2 &= L - q_2 \\ \left(r_2 + \frac{d}{2}\right)\theta_2 &= L - q_2 + \delta_2 \end{aligned} \tag{3}$$

Combining (1), (2) and (3) reveals that the curvatures (κ) of the two sections are equivalent, and independent of the location of the crossover point:

$$\kappa \triangleq \frac{1}{r_1} = \frac{1}{r_2} = \frac{2q_1}{dL} \tag{4}$$

With κ, ℓ_1, and ℓ_2 defining a configuration space for the manipulator, it is straightforward to convert to a space curve representation parameterized in arc length that will provide the Cartesian coordinates of the robot's tip or any other point along it [3].

Note that inserting or retracting one strip without changing the length of the other will result in a small amount of extension

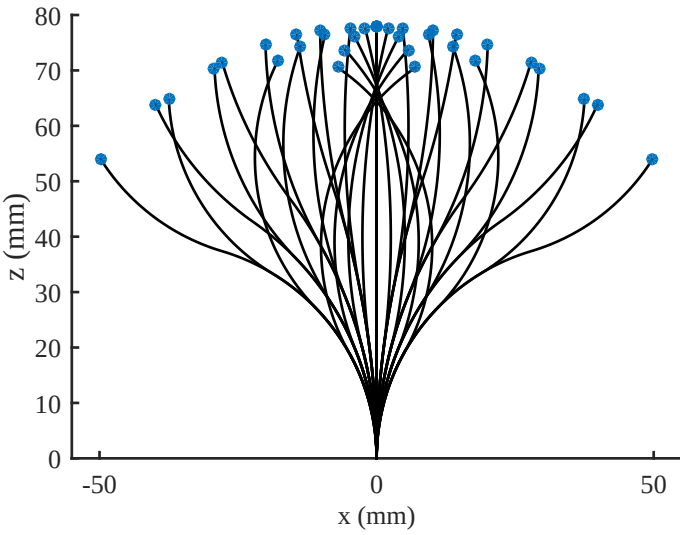

FIGURE 4: Demonstration of the workspace of the prototype robot.

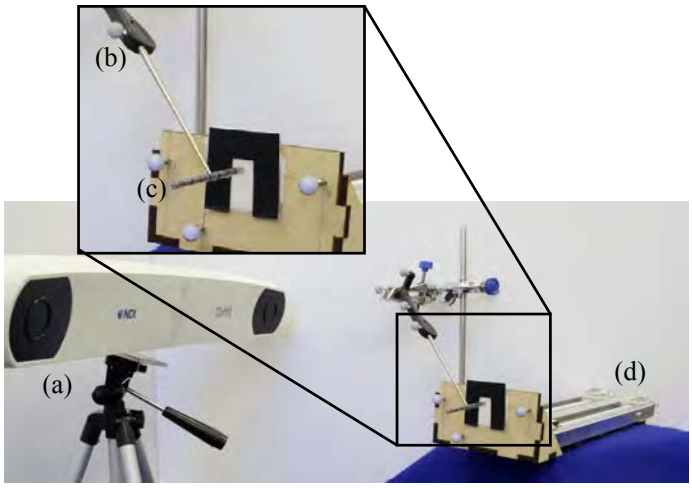

FIGURE 5: Experimental setup including (a) optical tracking system, (b) tracked probe, (c) prototype continuum robot, and (d) linear slide actuators.

FIGURE 6: Examples of the robot motion achieved with our experimental setup.

or contraction of the overall length L. Here, we assume that this effect is negligible, such that the model is symmetric for positive and negative values of q_1.

Based on this kinematic model, and assuming a range of allowable actuator values of -4 mm $< q_1 <$ 4 mm and 20 mm $< q_2 <$ 50 mm for the prototype described in the previous section, a sampling of the workspace of the robot is shown in Figure 4.

EXPERIMENTS

To validate the kinematic model described in the previous section, the experimental prototype was mounted to a base plate which was attached to a pair of precision linear positioning slides, as shown in Figure 5. One of these slides was used to control the insertion and retraction of one of the bending strips (q_1), while the other was used to control the position of the crossover disc (q_2). Examples of the motion resulting from these inputs are shown in Figure 6.

To obtain position data along the length of the robot, the Polaris Spectra optical tracking system (Northern Digital, Inc.) was used to track a point probe. A series of seven marks were drawn on the outside of the outer sheath of the manipulator, beginning 10 mm from the base plate. Nine data points were collected for each pose of the manipulator by carefully touching the tip of the tracked probe to the base of the robot, to each of the seven marked locations along the robot, and finally to the tip of the robot. Position values for these points were recorded with respect to a base frame defined by three markers rigidly attached to the base plate of the experimental setup.

A total of 35 actuator configurations were applied to the robot, and the resulting shape was recorded with the optical tracking system for each of these configurations. The values of q_2 tested were $q_2 = \{20, 25, 30, 35, 40, 45, 50\}$ mm, and the values of q_1 used for each of these crossover disc locations were $q_1 = \{-4, -2, 0, 2, 4\}$ mm.

The results of the experiment, shown in Figures 7, 8 and 9, demonstrate that the kinematic model is accurate throughout the range of actuator values tested in these trials. The overall

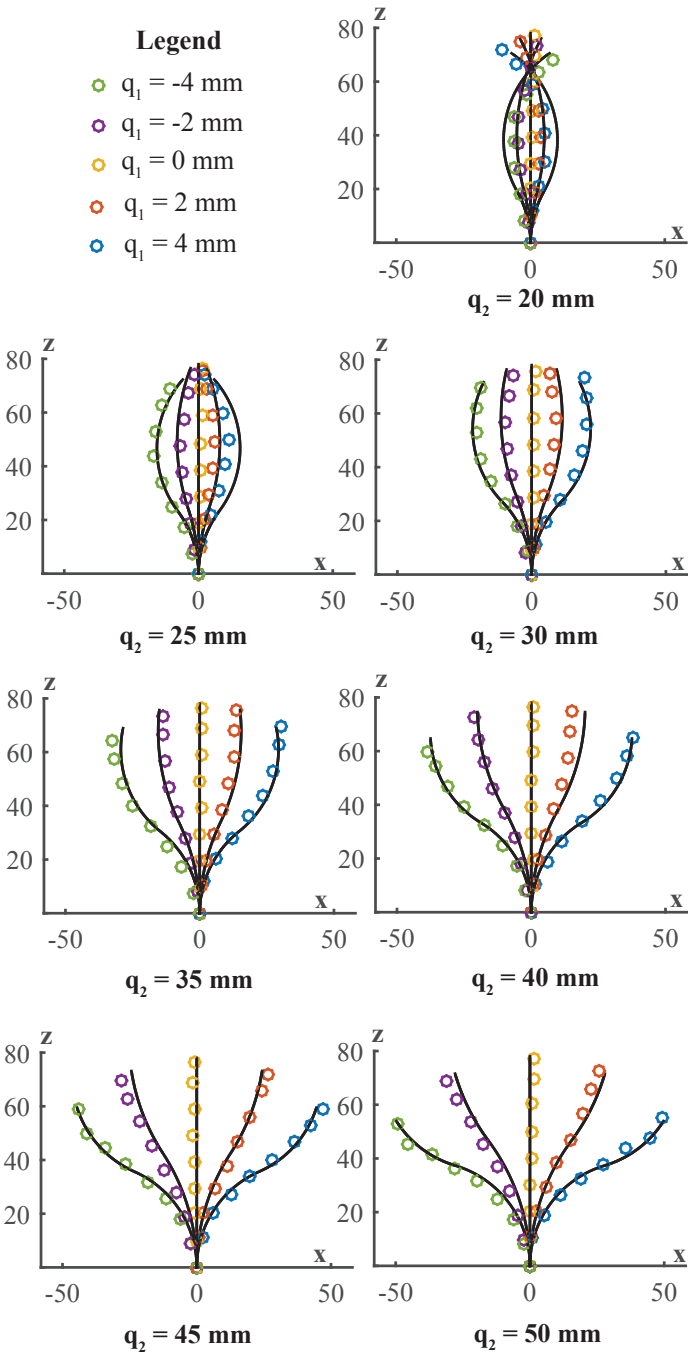

FIGURE 7: Results of experimental validation of kinematic model. The shape predicted by the model is shown in black and the experimentally observed shape is shown in colored circles.

average tip position error was 3.6 mm or 4.6% of the robot's length, while the worst tip position error observed in any single trial was 7.2 mm or 9.2% of the robot's length. The poorest tip accuracies were observed at the smallest values of q_2 tested, as shown in Figure 8.

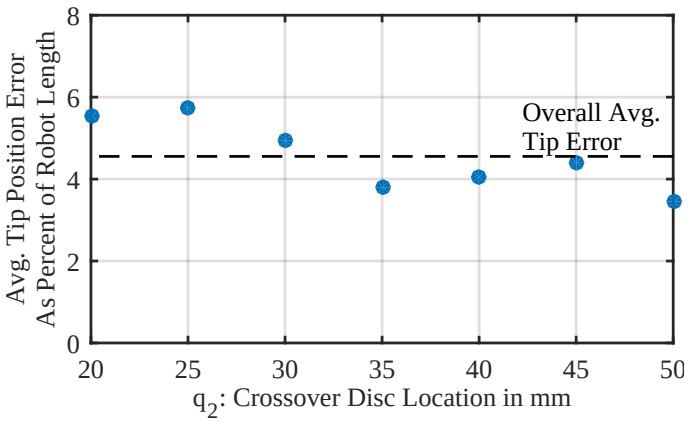

FIGURE 8: Model tip error, averaged over five values of q_1 tested, versus crossover disc location.

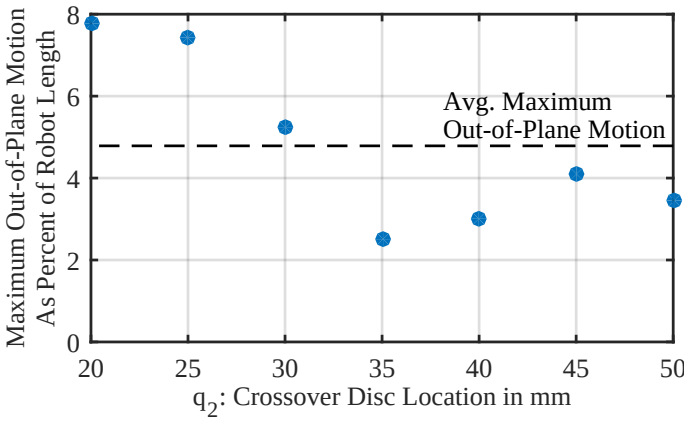

FIGURE 9: Maximum out-of-plane distance observed for any value of q_1 anywhere along the robot length versus crossover disc location.

A substantial portion of the model error comes from unintended out-of-plane motion, which is most significant when the crossover disc is positioned near the base. This effect is illustrated in Figure 9, which shows the maximum recorded out-of-plane motion observed anywhere along the robot's length for any tested value of q_1 as a function of the crossover disc location q_2. The pattern of out-of-plane motion mirrors that of the tip position error, with the highest degree of out-of-plane motion observed for the smallest values of q_2.

DISCUSSION AND CONCLUSIONS

In this paper, we have presented a new design for a two-section planar continuum robot whose relative section lengths

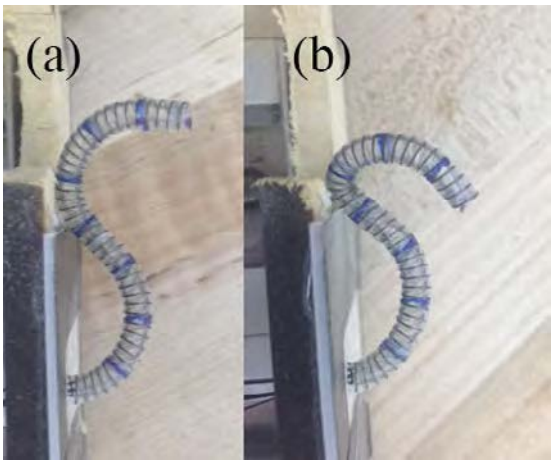

FIGURE 10: Test of robot bending capabilities. (a) shows the robot actuated until it comes in contact with the base plate, and (b) shows the robot after continued actuation, just prior to failure.

can be varied by one of the actuation inputs. A useful feature of this design is that it requires only one degree of freedom for bending and one degree of freedom for the adjustment of the point of curvature change between the two sections. This results in a robot with two coupled continuum sections of equal curvature that bend in opposite directions, where the sum of the sections' lengths is constant, but their individual lengths can vary. Axial rotation at the base of the robot can be used to obtain a spatial rather than planar workspace.

The simple geometry-based kinematic model presented in this paper is experimentally shown to be accurate for the robot configurations tested in the preceding section. Thus, depending on specific task requirements, this model may be sufficient. However, as the crossover point is brought closer and closer to the base, the model begins to lose accuracy and out-of-plane motion becomes significant.

The actuator limits defined for the model validation experiments are somewhat arbitrary, and were chosen in order to be confident that the robot will not be damaged as it is actuated, though inputs outside of the stated ranges are possible. In its straight configuration, it is possible to vary q_2 from 6 mm to 57 mm. However, at these extreme crossover disc locations, the amount of bending possible is much more limited, and the model proposed in this paper no longer predicts the robot shape well. To explore the limits on q_1, we positioned the crossover disc in approximately the middle of the robot length at $q_2 = 40$ mm, and began retracting the actuated strip as far as possible. As shown in Figure 10(a), the mechanism achieved a high curvature and remained in approximately circular arcs, bending far enough to come into contact with the frame holding it. Continuing to withdraw the strip after this point resulted in the pose shown in Figure 10(b), until finally the glue bonds between the crossover disc and the smaller strips failed at $q_1 = -16$ mm. This demonstrates that the robot has a usable workspace beyond the limits we chose in this paper. In contrast to q_2, we suspect that the model proposed in this paper would work well for a larger range of q_1. However, testing this is left to future work.

Frictional effects, which are assumed negligible in the model proposed in this paper, are also worthy of further discussion. Friction between the bending strips and the crossover disc would tend to make the strip distribute itself unevenly between the two sections of the robot. This would create a hysteresis in the manipulator pose and cause increased deviation from the model-predicted behavior. The prototype used in these experiments has not been optimized to minimize friction (in particular, there was a relatively tight tolerance between the crossover disc and the strips passing through it), and did exhibit some hysteresis. We sought to mitigate this effect in our experiments by oscillating q_1 by $\pm$ 1 mm around each actuator set point for approximately five cycles. It may be possible to reduce frictional effects in future design iterations by oversizing the slits in the crossover disc and using highly lubricious materials.

The constant overall length assumption used in this model is also a source of some of the tip position error. In order to better agree with the constant length assumption and achieve a more symmetrical workspace as the model predicts, an actuation scheme in which the two strips are translated by equal and opposite amounts may in fact be preferable. These two translations could be mechanically coupled to avoid the need for an additional actuator. Alternatively, the elongation and contraction of the length could be incorporated into the geometric model.

Another interesting option for future work would be to develop a mechanics-based model, which could potentially improve the accuracy of the planar kinematics, predict out-of-plane motion, and describe the behavior of the manipulator under known external loads. For example, a Cosserat rod-based modeling approach, which has been used in prior work for tendon-driven designs [24], concentric tube robots [16], and continuum parallel robots [25] could prove effective here.

Increasing the number of adjustable length sections within the manipulator is another area for future work. Assuming sufficient space within the cross-section of the robot, it is possible to add additional discs which cause the robot to cross in more than one location, thereby increasing the number of sections. In this case, the inclusion of n discs should result in $n+1$ different sections of adjustable length.

In summary, the new manipulator we describe in this paper offers the possibility of achieving a wider range of shapes with fewer actuators than prior continuum robots. We believe these capabilities may be useful in minimally invasive surgery and also in industrial inspection tasks. Also importantly, the work in this paper contributes a new design to the emerging subfield of continuum robots involving nonlinear actuation element routing (see e.g. [23,24,26]) – a powerful concept which we believe is poised

to enable new future applications and capabilities in continuum robots.

REFERENCES

[1] Robinson, G., and Davies, J. B. C., 1999. "Continuum robots–a state of the art". *Robotics and Automation, IEEE International Conference on*, pp. 2849–2854.

[2] Trivedi, D., Rahn, C. D., Kier, W. M., and Walker, I. D., 2008. "Soft robotics: Biological inspiration, state of the art, and future research". *Applied Bionics and Biomechanics,* **5**(3), pp. 99–117.

[3] Webster III, R. J., and Jones, B. A., 2010. "Design and kinematic modeling of constant curvature continuum robots: A review". *The International Journal of Robotics Research,* **29**(13), pp. 1661–1683.

[4] McMahan, W., Chitrakaran, V., Csencsits, M., Dawson, D., Walker, I. D., Jones, B. A., Pritts, M., Dienno, D., Grissom, M., and Rahn, C. D., 2006. "Field trials and testing of the OctArm continuum manipulator". *Robotics and Automation, IEEE International Conference on*, pp. 2336–2341.

[5] Ohno, H., and Hirose, S., 2000. "Study on slime robot (proposal of slime robot and design of slim slime robot)". *Intelligent Robots and Systems, IEEE/RSJ International Conference on*, pp. 2218–2223.

[6] Chen, G., Pham, M. T., and Redarce, T., 2006. "Development and kinematic analysis of a silicone-rubber bending tip for colonoscopy". *Intelligent Robots and Systems, IEEE/RSJ International Conference on*, pp. 168–173.

[7] Immega, G., and Antonelli, K., 1995. "The KSI tentacle manipulator". *Robotics and Automation, IEEE International Conference on*, pp. 3149–3154.

[8] Bailly, Y., Amirat, Y., and Fried, G., 2011. "Modeling and control of a continuum style microrobot for endovascular surgery". *Robotics, IEEE Transactions on,* **27**(5), pp. 1024–1030.

[9] Li, C., and Rahn, C. D., 2002. "Design of continuous backbone, cable-driven robots". *Journal of Mechanical Design,* **124**(2), pp. 265–271.

[10] Gravagne, I. A., Rahn, C. D., and Walker, I. D., 2003. "Large deflection dynamics and control for planar continuum robots". *Mechatronics, IEEE/ASME Transactions on,* **8**(2), pp. 299–307.

[11] Degani, A., Choset, H., Wolf, A., and Zenati, M. A., 2006. "Highly articulated robotic probe for minimally invasive surgery". *Robotics and Automation, IEEE International Conference on*, pp. 4167–4172.

[12] Camarillo, D. B., Milne, C. F., Carlson, C. R., Zinn, M. R., and Salisbury, J. K., 2008. "Mechanics modeling of tendon-driven continuum manipulators". *Robotics, IEEE Transactions on,* **24**(6), pp. 1262–1273.

[13] Kim, Y., Cheng, S. S., and Desai, J. P., 2015. "Towards the development of a spring-based continuum robot for neurosurgery". *SPIE Medical Imaging*, pp. 94151Q–94151Q.

[14] Simaan, N., Xu, K., Wei, W., Kapoor, A., Kazanzides, P., Taylor, R., and Flint, P., 2009. "Design and integration of a telerobotic system for minimally invasive surgery of the throat". *The International Journal of Robotics Research,* **28**(9), pp. 1134–1153.

[15] Dupont, P. E., Lock, J., Itkowitz, B., and Butler, E., 2010. "Design and control of concentric-tube robots". *Robotics, IEEE Transactions on,* **26**(2), pp. 209–225.

[16] Rucker, D. C., Jones, B. A., and Webster III, R. J., 2010. "A geometrically exact model for externally loaded concentric-tube continuum robots". *Robotics, IEEE Transactions on,* **26**(5), pp. 769–780.

[17] Walker, I. D., Carreras, C., McDonnell, R., and Grimes, G., 2006. "Extension versus bending for continuum robots". *International Journal of Advanced Robotic Systems,* **3**(2), pp. 171–178.

[18] Walker, I. D., 2013. "Robot strings: Long, thin continuum robots". *Aerospace Conference, 2013 IEEE*, pp. 1–12.

[19] Blessing, M., and Walker, I. D., 2004. "Novel continuum robots with variable-length sections". *Proc. 3rd IFAC Symp. on Mechatronic Syst*, pp. 55–60.

[20] Jones, B. A., and Walker, I. D., 2006. "Kinematics for multisection continuum robots". *Robotics, IEEE Transactions on,* **22**(1), pp. 43–55.

[21] Jones, B. A., and Walker, I. D., 2007. "Limiting-case analysis of continuum trunk kinematics". *Robotics and Automation, IEEE International Conference on*, pp. 1363–1368.

[22] Godage, I. S., Guglielmino, E., Branson, D. T., Medrano-Cerda, G. A., and Caldwell, D. G., 2011. "Novel modal approach for kinematics of multisection continuum arms". *Intelligent Robots and Systems, IEEE/RSJ International Conference on*, pp. 1093–1098.

[23] Yamada, A., Naka, S., Morikawa, S., and Tani, T., 2014. "MR compatible continuum robot based on closed elastica with bending and twisting". *Intelligent Robots and Systems, IEEE/RSJ International Conference on*, pp. 3187–3192.

[24] Rucker, D. C., and Webster III, R. J., 2011. "Statics and dynamics of continuum robots with general tendon routing and external loading". *Robotics, IEEE Transactions on,* **27**(6), pp. 1033–1044.

[25] Bryson, C. E., and Rucker, D. C., 2014. "Toward parallel continuum manipulators". *Robotics and Automation, IEEE International Conference on*, pp. 778–785.

[26] Zhang, J., and Simaan, N., 2013. "Design of underactuated steerable electrode arrays for optimal insertions". *Journal of Mechanisms and Robotics,* **5**(1), p. 011008.